Taylor's statistical theory applied to the turbulence parameterization in the BAM-INPE global atmospheric model

Eduardo Rohde Eras[1], Haroldo Fraga de Campos Velho[1], and Paulo Yoshio Kubota[1]

[1]Instituto Nacional de Pesquisas Espaciais (INPE), São José dos Campos - SP, Brazil

Correspondence: Eduardo Rohde Eras (eduardo.eras@inpe.br)

Abstract. Turbulence parameterization scheme for planetary boundary layer (PBL) based on Taylor's statistical formulation for turbulent flow is used in the Brazilian Global Atmospheric Model (BAM). Taylor's approach has been already applied to mesoscale and air pollution atmospheric models, but it is the first time that this approach is employed in a global model. The BAM model is operationally used to generate numerical weather forecasting by the INPE (National Institute for Space Research – Brazil). The simulation performed with BAM model using Taylor's parameterization is compared with the results obtained with the schemes presented by Holtslag-Boville, Sungsu-Park, and Mellor-Yamada trying to reproduce the ERA5 reanalysis data of two different initial conditions of two different seasons (dry season and wet season). The obtained comparison exhibit a positive result for the new parameterization simulating global precipitation, cloud coverage, and top atmospheric thermal radiation, specially in the dry season. Positive results for the Amazon basin were also obtained.

1 Introduction

Turbulence is a permanent feature in the dynamic of the atmosphere. The closest layer to the ground is the region called the *planetary boundary layer* (PBL), where the turbulence must be represented. The production of turbulence in the PBL is associated with wind shear or transport of thermal energy between the ground and the atmosphere. If the ground temperature is lower than the atmosphere temperature, there will be a heat flow from the atmosphere to the ground, removing energy from the PBL, a situation commonly found during the night. On the other hand, when the surface temperature is greater than the atmosphere – for instance, during the day time – a thermal flux from the land can be established generating a convective boundary layer (STULL, 1988). Different stability conditions for the PBL can be typified by calculating the Monin-Obukhov length.

The complete understanding about the turbulence is a challenge for modellers. However, a representation for the turbulent flow is essential to be included in the computer programs for numerical weather prediction (NWP). One approach is to consider the Reynolds' assumption, where those fluid properties can be expressed as the summation of an mean value for the physical property (flowing in a similar way such as a laminar flux) added to a stochastic forcing. The average of the random forcing

is assumed as zero, but the product between two of these stochastic variables is not null. Indeed, the product of each two
25 random variables is named as *Reynolds tensors* (FOKEN , 2017), From this consideration, the goal becomes how to express
the Reynolds tensors as a function of the mean atmospheric variables.

These tensors are parameterized to represent turbulence in a simulation software. Turbulence parameterization has been
investigated using different closing approaches (STULL, 1988) and different closing orders, either first order (DEGRAZIA et
al., 2000; HOLTSLAG-BOVILLE, 1993), or higher orders (MELLOR-YAMADA, 1982). Turbulent modeling based on Tay-
30 lor's formulation has already been applied to the atmospheric pollutant models: Lagrangian (ROBERTI et al. , 2005), Eulerian
(CARVALHO et al., 2002), and Gaussian (RIZZA et al. , 2001) ones, and atmospheric mesoscale models: BRAMS (**B**razilian
developments on the **R**egional **A**tmospheric **M**odeling **S**ystem) (BARBOSA et al., 2011) – see: `http://brams.cptec.inpe.br/`
– and METRAS (**ME**soskaliges **TRA**nsportund **S**trömungsmodell) (SCHUNZEN, 1994) – see: `https://mi-pub.cen.uni-`
`hamburg.de/index.php?id=3`
35 `59`.

This article describes the results with the implementation of the turbulence parameterization based on Taylor's theory (1922)
for different PBL stability conditions in the BAM model (Brazilian global Atmospheric Model) -– see Figueroa *et al*. (2016).
Here is the first time that Taylor's theory on turbulence is applied to a global model of atmospheric dynamics. It's particularly
desired to evaluate the parameterization results for the Amazon basin, given its important climatic influence in neighbour
40 regions, specially for weather forecast in the southeast part of Brazil (YANG, 2019; LEMES et al., 2020)

The results with the new parameterization are compared with the schemes presented by Holtslag-Boville (1993), Sungsu-
Park (2009), and Mellor-Yamada (1982), to represent the turbulence.

2   The Brazilian Atmospheric Model

The National Institute of Space Research (Instituto Nacional de Pesquisas Espaciais - INPE) is responsible for the opera-
45 tional execution of numerical weather forecasting, climate forecasting and environmental forecasting models. The BAM model
(FIGUEROA et al., 2016) is a 3-dimension hydrostatic code with two formulations of dynamic kernel (Eulerian and semi-
Lagrangian), where the equations are spatially discretized using a spectral method, developed for numerical weather forecast-
ing, simulations and climate forecasts (COELHO et al., 2021). According to FIGUEROA et al. (2016), the global model was
entirely developed to be used on time scales ranging from days to seasons, and in horizontal resolutions in the order of 10km
50 to 200km. The model can be used either for deterministic numerical weather forecasting on the 1 to 10 day scale, probabilistic
extended numerical weather forecasting on the 1 to 4 week scale (when coupled with an ocean model), or even as a complete
earth simulation model for forecasting seasonal climate and climate change studies. During INPE's operation, the model runs
with a spatial resolution of approximately 20 kilometers, with 64 vertical levels and a semi-Lagrangian semi-implicit scheme
for time integration. Among others, the BAM model provides data to the National Electric System Operator (ONS, 2022) and
55 the Cearense Foundation of Meteorology and Artificial Rainfall (FUNCEME, 2022).

In the global model of atmospheric dynamics adopted by INPE for numerical weather forecasting, first and second order PBL parameterizations were implemented, which currently include three different options:

1. The Holtslag-Boville first order representation of turbulent flows (HOLTSLAG-BOVILLE, 1993) takes into account a counter gradient term (computed for convective layer), modeling local and non-local scheme for vertical diffusion.

60
2. The University of Washington Moist Turbulence (UWMT) developed by Christopher S. Bretherton and Sungsu Park (SUNGSU-PARK, 2009) is a first order moist turbulence parameterization improved for numerical stability and efficiency with the long time steps used in climate models, with a original goal to provide a more physically realistic treatment of marine stratocumulus-topped boundary layers.

3. The Mellor-Yamada second order PBL turbulence model (MELLOR-YAMADA, 1982) an experience realised at Prince-
65
ton University, is the result of a collection of studies carried by the authors and others that culminated in a set of physical models based on hypotheses by Rotta and Kolmogorov.

3 Turbulence parameterization from the Taylor's statistical theory

As expressed by the gas kinetic theory, the diffusion coefficient is proportional by the product between a characteristic speed ($\langle v \rangle$) and a characteristic length (ℓ) (ROBERTS-WEBSTER, 2002). Taking this into account, the British physicist and mathe-
70
matician Geoffrey Ingram Taylor published a paper entitled *Diffusion by Continuous Movements* (1922), founding the basis for his statistical theory of turbulence. In the formulation based on Taylor's approach, the displacement x between two particles embedded in a turbulent flow can be written as (BATCHELOR, 2008):

$$\frac{d\langle x^2(t) \rangle}{dt} = 2 \langle v^2(t) \rangle \int_0^t \rho(\tau)\, d\tau \qquad (1)$$

where the self-correlation function is denoted by $\rho(\tau) \equiv [\langle v(t)\, v(t+\tau) \rangle] / \langle v^2(t) \rangle$, and $v(t)$ is a random fluctuation for the
75
velocity. Integrating by parts equation (1), the fundamental equation to the Taylor's formulation describing a property for turbulent flow is derived:

$$\langle x^2(t) \rangle = 2 \langle v^2(t) \rangle \int_0^t (t-\tau)\rho(\tau)\, d\tau \, . \qquad (2)$$

However, a turbulence representation is obtained by using the the Fourier transform / anti-Fourier transform pair of the correlation function 2. Therefore, an expression for the spacing of fluid parcels is obtained with a spectral form:

80
$$\langle x^2(t) \rangle = \sigma_i^2 t^2 \int_0^{+\infty} F_{L_i}(n) \left[\frac{\sin^2(\pi n t)}{(\pi n t)^2} \right] dn \qquad (3)$$

where σ_i^2 is the variance of wind speed, F_{L_i} is the Lagrangian non-dimensional spectrum and the frequency n is given in Hertz – instead of radians/second ($\omega = \mathrm{rad}/s$), where $n = \omega/2\pi$. However, most observations in meteorology are collected by

Geoscientific
Model Development
Discussions

Eulerian flow approach instead of Lagrangian one. Then, the Gifford-Hay and Pasquill hypothesis $\rho_{L_i}(\beta_i \tau) = \rho_i(\tau)$, where ρ_i is an Eulerian correlation function and β_i is the relationship between the Lagrangian and Eulerian decorrelation scales. With a change of variables, and employing an expression derived by Batchelor (1949) to the eddy diffusivity:

$$K_{\alpha\alpha} = \frac{1}{2}\frac{d\sigma_i^2}{dt} \tag{4}$$

with σ_i^2 the variance for the velocity component ($i = u, v, w$), and α identify the different space direction ($\alpha = x, y, z$), it can be combined with Eq. (3) to derive an expression for the turbulent diffusivity (DEGRAZIA–MORAES, 1992; DEGRAZIA et al., 1997):

$$K_{\alpha\alpha} = \frac{\sigma_i^2 \beta_i}{2\pi} \int\limits_0^{+\infty} F_i(n) \frac{\sin(2\pi n t/\beta_i)}{n}\, dn \tag{5}$$

where $\alpha = (x, y, z)$ is the turbulent diffusivity direction, $i = (u, v, w)$ is the wind velocity direction, σ^2 is the wind velocity variance, $\beta_i = \left[(\pi U^2)/(16\,\sigma_i^2)\right]^{1/2}$ is the ratio between the scale of the Lagrangian and Eulerian spectra, $F_i(n)$ is the Eulerian dimensionless spectrum of kinetic energy, n is a dimensionless frequency, and t is time.

3.1 The turbulence parameters

For long travel times $t \to \infty$, an asymptotic behavior for Eq. (5) can be derived resulting:

$$K_{\alpha\alpha} = \frac{\sigma_i^2 \beta_i F_i(0)}{4} \tag{6}$$

where $K_{\alpha\alpha}$ is the turbulent diffusivity in any direction, and $F_i(0)$ is the non-dimension spectrum in the origin. Based on the relationship between the turbulence parameters $K_{\alpha\alpha} = \sigma_i^2 T_{L_i} = \sigma_i \ell_i$ an expression for Lagrangian decorrelation scale (T_L) is found:

$$T_{L_i} = \frac{\beta_i F_i(0)}{4}\ . \tag{7}$$

Similarly, an expression for the mixing length is found:

$$\ell_i = \frac{\sigma_i \beta_i F_i(0)}{4} \tag{8}$$

3.1.1 Stable Boundary Layer (SBL) and Neutral Boundary Layer (NBL)

With appropriate expressions for the spectra, it is possible to describe formulations for each type of stability in the PBL (DEGRAZIA–MORAES, 1992). Using the so-called Monin-Obukhov local similarity theory adjusted for SBL and NBL, a general expression for the dimensionless turbulent velocity spectrum in the surface boundary layer (OLESEN et al., 1984) where the experimental constants are derived for the desired type of stratification, and also considering Kolmogorov's law in the inertial subdomain with local similarity, the variance of the wind velocity and the dimensionless spectrum in the Origin for

the SBL and NBL. Nieuwstadt (1984) adapted the similarity theory for the stable boundary layer, where the wind shear (τ),

110 heat flux ($\overline{w'\theta'}$), and local Monin-Obukov length (Λ) are expressed by

$$\frac{\tau}{\tau_0} = \frac{U_*^2}{u_*^2} = (1 - z/h)^{\alpha_1} \;;$$

$$\frac{\overline{w'\theta'}}{(\overline{w'\theta'})_0} = (1 - z/h)^{\alpha_2} \;;$$

$$\frac{\Lambda}{L} = (1 - z/h)^{3\alpha_1/2 - \alpha_2} \;.$$

Using the formulation presented in the Equation 6, an expression for the turbulent diffusivity for the SBL and NBL is given

115 by:

$$\frac{K_{\alpha\alpha}}{u_* h} = \frac{\sqrt{\pi}}{16} \frac{0.64 \, (2.33 c_i)^{1/2}}{(f_m)_{n,i}^{4/3} \, c_\varepsilon^{-1/3}} \frac{[1 - (z/h)^{\alpha_1/2} \, (z/h)}{1 + 3.7(z/h)\,(h/\Lambda)} \tag{9}$$

where h is the PBL height, $u = \sqrt{\tau_s/\rho_{air}}$ is a velocity scale (*friction velocity*), Λ is the local Monin-Obukhov length, f_m is the spectral maximum calculated using the constants c_ε, and $c_i = \alpha_i a_1 (2\pi k)^{-2/3}$ in the $i \in (u, v, w)$ directions. For neutral boundary layer, the exponents $\alpha_1 = 2$, and $\alpha_2 = 3$ were estimated from the Minnesota experiment (KAIMAL; WYNGAARD,

120 1990), values $\alpha_1 = 3/2$ and $\alpha_2 = 1$ are applied to the stable boundary layer, results from the Cabauw experiment (MONNA; VAN DER VLIET, 1987).

Joining the appropriate turbulence parameters and experimental data, the vertical diffusion coefficient for the turbulence in the SBL and NBL yields (DEGRAZIA–MORAES, 1992):

$$\frac{K_{zz}}{u_* h} = \frac{0.33\,[1 - (z/h)]^{\alpha_1/2}\,(z/h)}{1 + 3.7\,(z/h)\,(h/\Lambda)} \;. \tag{10}$$

125 ### 3.1.2 Convective Boundary Layer (CBL)

Using a convective velocity length based on heat flux $(\overline{w'\theta'})_0$ between surface and atmosphere, the Monin-Obukhov length is calculated for the CBL. Also, a spectrum model with the convective velocity scale calculated from the general expression for the dimensionless turbulent velocity spectrum alongside Kolmogorov's law for the inertial subdomain formulated in terms of convective similarity parameters is used to derive the spectrum for the CBL. From the definition presented in the Equation 6,

130 using the Variance of the Wind Velocity and the Dimensionless Spectrum in the Origin for the CBL, an expression for turbulent diffusivity $K_{\alpha\alpha}$ for CBL is seen in equation below (DEGRAZIA et al., 1997):

$$\frac{K_{\alpha\alpha}}{w_* h} = \frac{1.5^{5/6} \kappa^{1/3} c_i^{1/2} \sqrt{\pi}}{16} \frac{\psi^{1/3} (\lambda_m)_i^{4/3}}{h^{1/3}} \tag{11}$$

where $w_* = \left[(g/\theta_0)\,(\overline{w'\theta'})_0\,h\right]$ is a convective velocity scale, $\kappa = 0.4$ is the *von Kármán* constant, $c_i = \alpha_i a_1 (2\pi\kappa)^{-2/3}$ is calculated using convective constants derived from the Minnesota and Cabauw experiments, $\psi = [(\varepsilon h)/(w_*^3)]$ is a dimensionless

135 dissipation function, λ_m the wavelength value for the spectral peak, and h is the PBL height.

Using the convective diffusivity from the Equation 11 and the appropriate convective experimental data, the vertical diffusion seen in Equation 12 model the turbulence for the CBL (DEGRAZIA et al., 1997):

$$\frac{K_{zz}}{w_* h} = 1.16 \, \psi^{1/3} \left[1 - \exp\left(-4\frac{z}{h}\right) - 0.0003 \exp\left(8\frac{z}{h}\right) \right]^{4/3} . \tag{12}$$

3.2 Modeling different PBL stability conditions

140 To calculate the three different PBL stability conditions supported by the Taylor parameterization, an update to the model was made by implementing a decision based on the *stability parameter*, consisted by the height z divided by the Obukhov length L. Given the definition:

$$L = -\frac{u_*^3}{\kappa \beta_c q_*} \tag{13}$$

where q_* is the vertical head flux, is possible to define unstable PBL when the Obukhov length is negative and stable PBL

145 for positive Obukhov lengths. However, neutral condition theoretically happens when there is no vertical heat flux, i.e. when q_* approaches to zero, consequently making the length L converges to infinity. To simulate infinity and division by zero, a threshold was established defining the neutral condition to happen when z/L is between -0.001 and 0.001.

Algorithm 1 Taylor parameterization PBL Stability Condition

1: stability_threshold = 0.001

2: **if** $z/L < -$ stability_threshold **then**

3:     stability = 'UNSTABLE'

4: **else if** $z/L >$ stability_threshold **then**

5:     stability = 'STABLE'

6: **else**

7:     stability (i) = 'NEUTRAL'

8: **end if**

---

4   Experiment and Model Configuration

Towards evaluate the Taylor based PBL parameterization, a set of simulations was conducted using the BAM model and the

150 results were compared with the reanalysis data from *ERA5 hourly data on single levels from 1959 to present* (HERSBACH et al., 2018). The simulations contemplated two different initial conditions, one at January (the wet season in the Amazon basin), and the second at September (the dry season in the Amazon basin). For each initial conditions, two different simulations were conducted: one 7 days (168 hours) simulation using the TQ62 triangular truncation horizontal resolution (approximately 215km), and the second in the TQ126 triangular truncation horizontal resolution (approximately 106km), booth using 28 ver-

155 tical sigma-layers. All the atmospheric simulations was realized using the BAM model in Eulerian mode. Four different PBL parameterizations was used in the simulations: Holtslag-Boville, Bretheron-Park, Mellor-Yamada, and the Taylor parameterization, presented in this paper. Beyond the PBL, other parameterizations are present in the model, including:

Table 1. Simulation Variables names and its units for the BAM model and its equivalent ERA5 reanalysis counterpart.

BAM		ERA5	
Variable Name	Unity	Variable Name	Unity
time mean temperature at 2m	K	2 meter temperature	K
planetary boundary layer height	m	boundary layer height	m
outgoing long wave at top	Wm^{-2}	top net thermal radiation	Jm^{-2}
cloud cover	ND	total cloud cover	$[0,1]$
total precipitation	$kg(m^2 \times day)^{-1}$	mean total precipitation rate	$kg(m^2 \times s)^{-1}$

– Gaseous absorption parameterization for shortwave (SW) radiation and long-wave (LW) radiation: CLIRAD (TARASOVA, FOMIN, 2007);

160 – Cumulus Parameterization: Arakawa-Schubert (RANDALL; PAN, 1993);

– Ocean model: slab (forced fixed condition in which all quantities are assumed to be completely and instantaneously homogenized (AMS, 2022));

– Snow model: Simplified Simple Biosphere SSiB (XUE et al., 1991);

– Soil-vegetation-atmosphere scheme: Integrated Biosphere Simulator Model IBIS (FOLEY et al., 1996).

165   The objective of this work is to evaluate the model performance reproducing the weather in the Brazilian rain forest. The initial conditions were generated from ERA5 hourly data in two different dates, named after the rainy (summer) and dry seasons in the Amazon basin:

– "dry" season: September 15, 2012;

– "wet" season: January 15, 2012.

170 Following the dry and wet initial conditions 16 simulations were realized, with two different lengths/resolutions for two different seasons and four different PBL parameterizations. Five simulation variables were chosen to compare the results from the BAM model with the ERA5 reanalysis, the name and its correspondent physical unit is shown in the Table 1.

All the simulations were evaluated in three different geographic areas: the Global (GBL), comprehending the entirely world; the Full South America (FSA) using latitude -60 to 15 and longitude -85 to 30; and the Amazon (AMZ) using latitude -12.5 to

175 0 and longitude -70 to -50.

Each one of the five BAM variables were compared with its respective ERA5 variable using three different error calculations, were a is the ERA5 variable and b is the BAM variable:

Geoscientific
Model Development
Discussions

– **Mean Relative Error (MRE):** gives the percentage difference in relation to ERA5 data:

$$MRE(a,b) = \frac{1}{N} \sum_{i=0}^{N} \frac{|a_i - b_i|}{|a_i|} \ . \tag{14}$$

– **Mean Difference (MD):** gives the sub-estimation or the super-estimation BAM output in relation to ERA5 data using the same physical units:

$$MD(a,b) = \frac{1}{N} \sum_{i=0}^{N} (a_i - b_i) \ . \tag{15}$$

– **Rooted Mean Square Error (RMSE):** gives the real (absolute) error in the same physical units of the original data. This is the chosen error calculation to evaluate most of the experiment:

$$RMSE(a,b) = \left[\frac{1}{N} \sum_{i=0}^{N} (a_i - b_i)^2 \right]^{\frac{1}{2}} \ . \tag{16}$$

5 Results

For the dry and wet seasons, the results obtained with the simulations configured with different horizontal resolutions and with the four PBL closing parameterizations were analyzed, comparing them with the ERA5 data for five different variables, in three different geographic ranges and using three different error calculations, totaling 720 sets of results. In this section, a brief overview of the simulated maps for each variable will be exposed, then the scenarios were the Taylor's PBL parameterization stood out will be addressed, first separated by season and simulation variable, then separated by geographic range.

5.1 The simulated maps

The two sets of data, the one simulated by the BAM model (in this section, always using the Taylor PBL parameterization) and the ERA5 reanalysis data, can be plotted on the terrestrial globe and visually compared. An example is the Cloud Cover map (Figure 1), where one can clearly see the similarities between the 12-hour forecast simulations performed by the model and the ERA5 reanalysis data. However, there is an overestimation of the Cloud Cover field, which may be related to greater stability of the nocturnal boundary layer simulated by the BAM model. In other words, the wind intensity in the boundary layer (1000 to 850 mb) must be weak and produce little mechanical turbulence, favoring the process of saturation and cloud formation.

The distinct selection of color palettes for each variable helps to highlight the differences in the amounts predicted by the model. Thus, some differences between the predicted variables and the reanalysis data variables may present abrupt color changes. The thermal radiation field emerging at the top of the atmosphere simulated by the model after 72 hours of the initial condition, seem in Figure 2, shows a difference in intensity especially in the convective systems of the tropical and subtropical region between the simulated field in 2a and the reanalysis data in 2b. But despite the small difference in intensity, the BAM model correctly simulated the pattern of the thermal radiation field emerging at the top of the atmosphere and the position of convective systems.
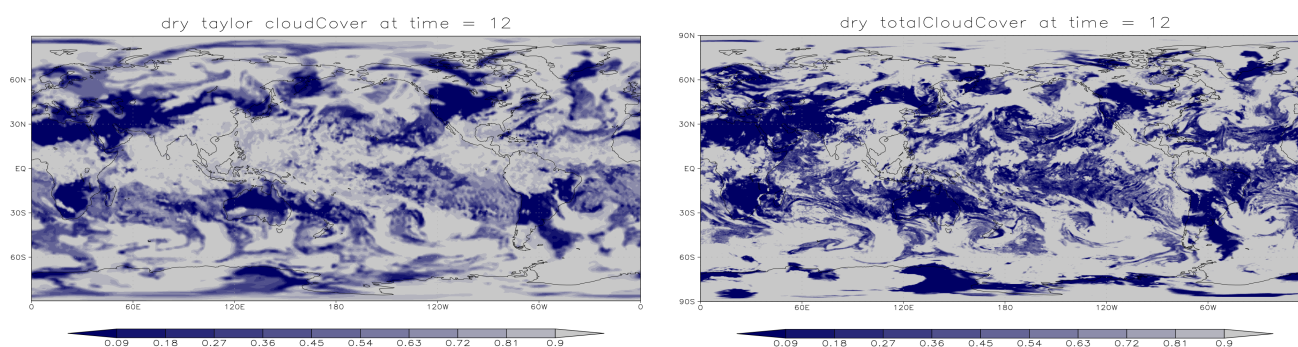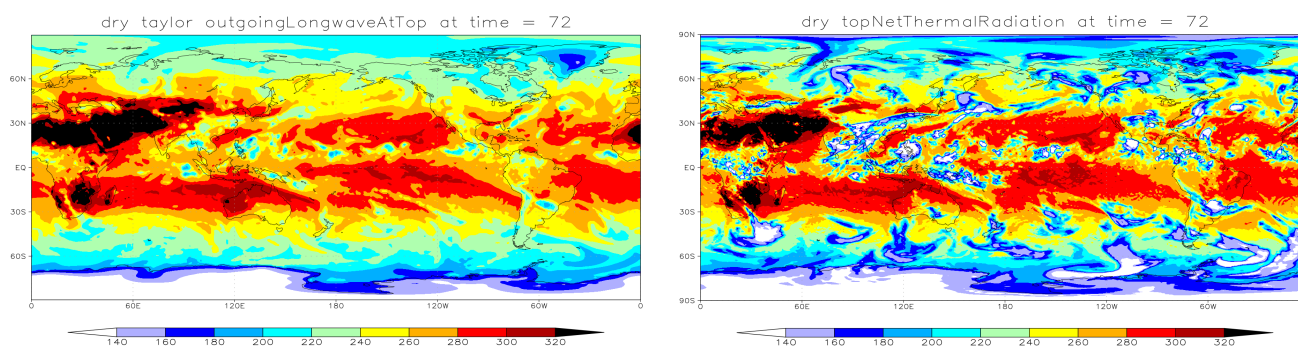
(a) Taylor's parameterization in BAM simulation at TQ126e.

(b) ERA5 reanalysis data.

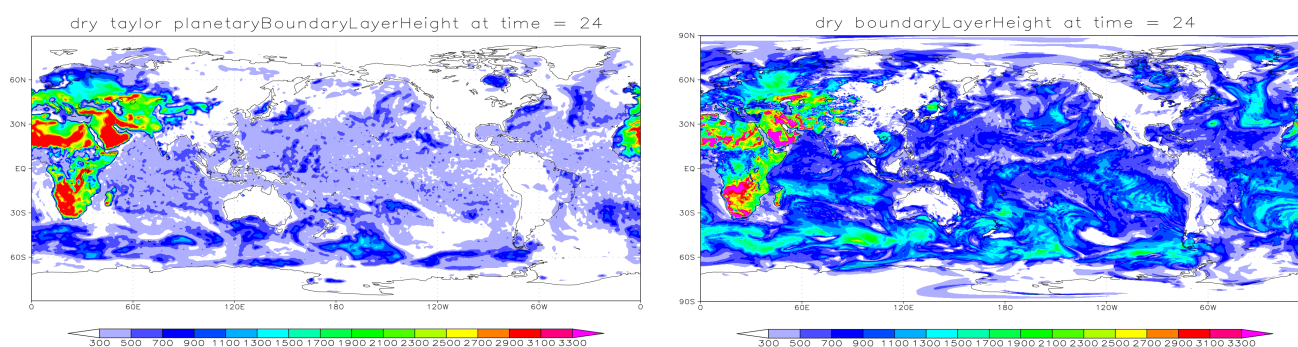**Figure 1.** Global Cloud Cover map in dry season after 12h from the initial condition.

(a) Taylor's parameterization in BAM simulation at TQ126e.

(b) ERA5 reanalysis data.

Figure 2. Global Long Wave (heat) Radiation at Top map in dry season after 72h from the initial condition.

The 3 illustrates the PBL height field map, where it is verified that the model consistently simulates the convective boundary layer during the day. However, at night, the model has difficulty simulating the height of the boundary layer in relation to the ERA5 reanalysis data. Analysing the general aspects of 3a and 3b, it appears that the height of the simulated PBL is generally underestimated compared to the ERA5 data. However, the correct position of the maximum and minimum height of the PBL

210 simulated by the BAM model is observed in comparison with the reanalysis data. This PBL height pattern partly explains what happens in the cloud cover field.

The map of the temperature field at 2 meters 4, are forecasts for 72 hours of forecast. In general, the magnitude of temperature is similar in most of the terrestrial globe. However, over the Tropical Atlantic, Tropical Pacific and Indian Oceans there is a temperature difference of up to a few degrees. This temperature pattern at 2 meters indicates that the sea surface temperature

215 used in the simulations is colder in relation to the ERA5 reanalysis data. Thus, as a consequence of the colder sea surface temperature used in the integration of the model, some meteorological systems may be affected such as tropical convection,

(a) Taylor's parameterization in BAM simulation at TQ126e.

(b) ERA5 reanalysis data.

Figure 3. Global PBL Height map in dry season after 72h from the initial condition.
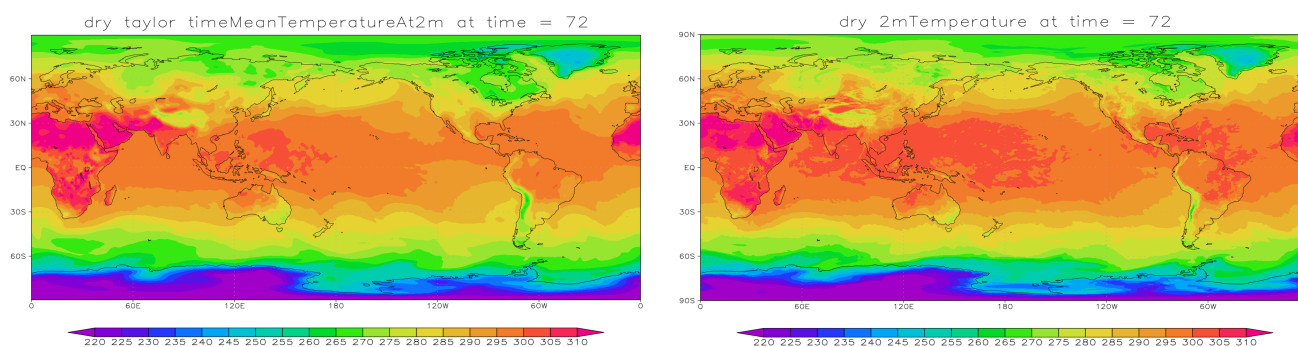
(a) Taylor's parameterization in BAM simulation at TQ126e.
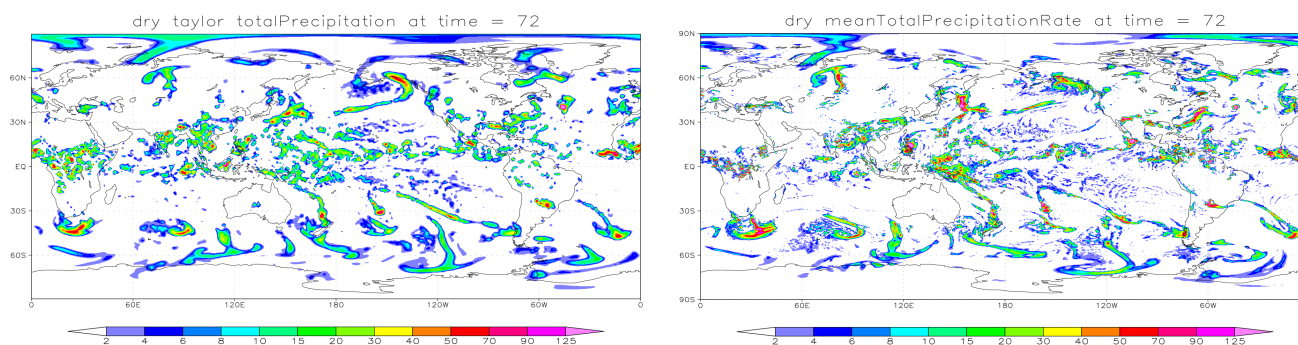
(b) ERA5 reanalysis data.

Figure 4. Global Mean Temperature at 2 meters map in dry season after 72h from the initial condition.

atmospheric saturation, the cloud cover field, and the interaction of radiation with the atmosphere. In South America, in some regions the forecast of the temperature at 2 meters is also overestimated by the BAM model.

220   The most interesting result for a weather forecast model is the simulated precipitation. In Figure 5a, the precipitation field after 72 hours of forecast is illustrated alongside the ERA5 data in Figure 5b, where it is verified that practically all the precipitating systems in the terrestrial globe are simulated consistently by the BAM model. However, the precipitation intensity of convective systems is underestimated by the BAM model. This may be related to the spatial and vertical resolution of the model, as well as aspects of the variables discussed earlier.

5.2   Dry Season

225   The simulation for the dry season obtained the best results for Taylor PBL parameterization. The largest number of variables and the most expressive advantages are discussed in the following sections.

(a) Taylor's parameterization in BAM simulation at TQ126e.

(b) ERA5 reanalysis data.

Figure 5. Global Mean Total Precipitation map in dry season after 72h from the initial condition.

5.2.1 Time Mean Temperature at 2m

The average temperature at 2 meters is not the best simulated variable with the Taylor parameterization, except in the Amazon. The average temperature at 2 meters is best simulated by the Park parameterization in most scenarios, but in the Amazon basin it was best simulated using the Taylor parameterization in both seasons, especially in the first week, as shown in Figure 6, where the shorter peaks (closer to K error) belongs to Taylor's, represented in black line.
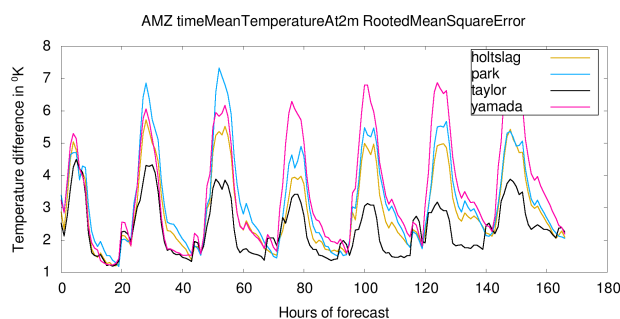
Figure 6. Time Mean Temperature at $2m$ in the Amazon basin, RMSE from BAM simulation at TQ62 in dry season compared to ERA5 reanalysis data.

### 5.2.2 Planetary Boundary Layer Height

The PBL height was better simulated by Holtslag and Park parameterizations in all scenarios. The Amazon basin region was where Taylor parameterization got its best approximations comparing to the ERA5 reanalysis data (see Tables 2, 3 and 4). During the dry season, the results from Taylor are almost indistinguishable from Park (Figure 7), a close second place towards the lower difference.
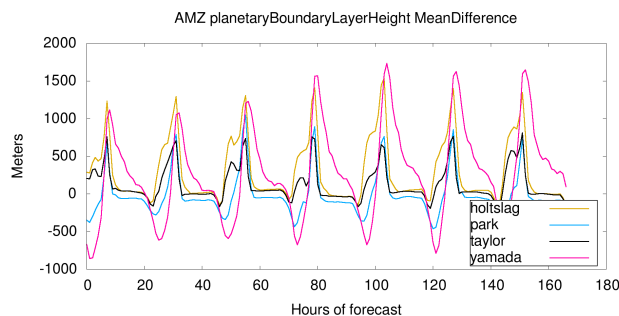
Figure 7. Planetary Boundary Layer Height in the Amazon basin, MD from BAM simulation at TQ62 in dry season compared to ERA5 reanalysis data.

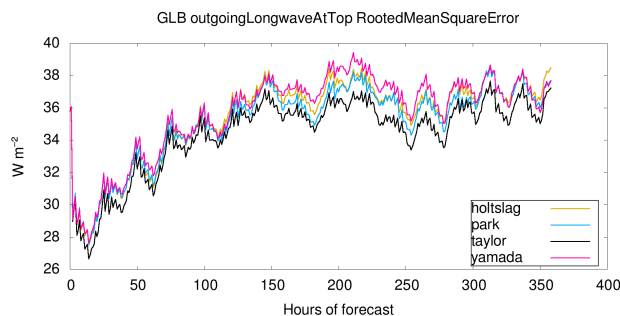### 5.2.3 Outgoing Long Wave at Top

The thermal radiation emitted into space at the top of the atmosphere simulated with the BAM model has a smaller error compared to the ERA5 reanalysis using Taylor PBL parameterization. The other PBL parameterizations present similar scenarios but with greater error. Figure 8 shows a lower significant error for the Taylor simulation in all three geographic regions: Global (GBL), over the territory of "Full" South America (FSA) and Amazon (AMZ). In Figure 9, the time series of thermal radiation emitted into space at the top of the atmosphere for each PBL method are plotted. The simulation obtained with the Taylor parameterization has the values at the bottom during the two simulated weeks, keeping the smallest error.
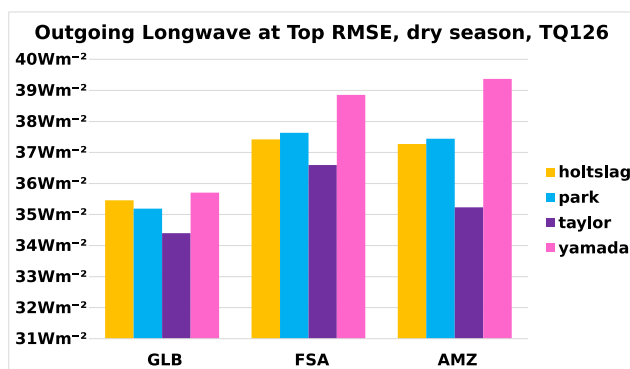
Figure 8. Outgoing Long Wave at Top, RMSE from BAM simulation at TQ126 in dry season compared to ERA5 reanalysis data in the three geographic ranges.
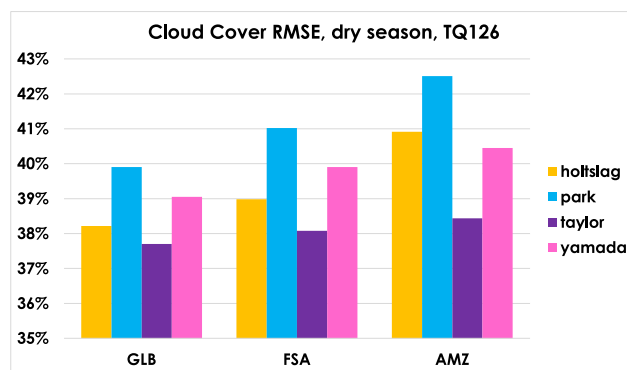
5.2.4 Cloud Cover

In Figure 9 it can be seen that cloud cover was best simulated during the dry season using Taylor PBL parameterization. The three geographic regions (GBL, FSA and AMZ) in Figure 10 indicate that Taylor PBL parameterization contributes to the

Figure 9. Global Outgoing Long Wave at Top, RMSE from BAM simulation at TQ126 in dry season compared to ERA5 reanalysis data.

reduction of cloud cover error in different regions of the globe in relation to the other boundary layer schemes. The Figure 11 is the cloud cover forecast time series, where it is verified that after the first week the Taylor parameterization presents a smaller error in relation to the other boundary layer schemes. Determining the influence of the boundary layer on the cloud cover field is very complex, as cloud formation depends on the interaction of many physical processes.


Figure 10. Cloud Cover, RMSE from BAM simulation at TQ126 in dry season compared to ERA5 reanalysis data in the three geographic ranges.

5.2.5 Total Precipitation

Precipitation is generally well represented by Taylor parameterization, especially in the dry season simulation. The difference in relation to the other methods is small, but it is indeed relevant given the importance of the variable. The Figure 12 illustrates the time series of the global MRE, where it can be seen that the results with the smallest error were obtained by the simulation using Taylor PBL parameterization.
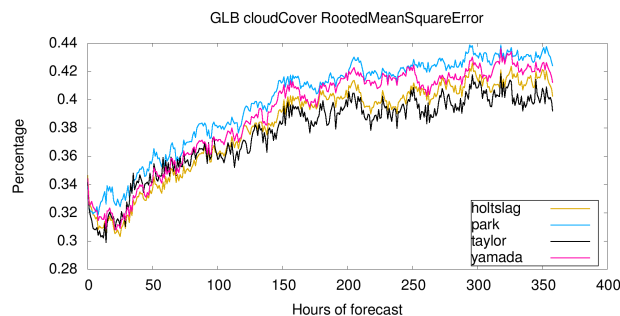
**Figure 11.** Global Cloud Cover, RMSE from BAM simulation at TQ126 in dry season compared to ERA5-5.
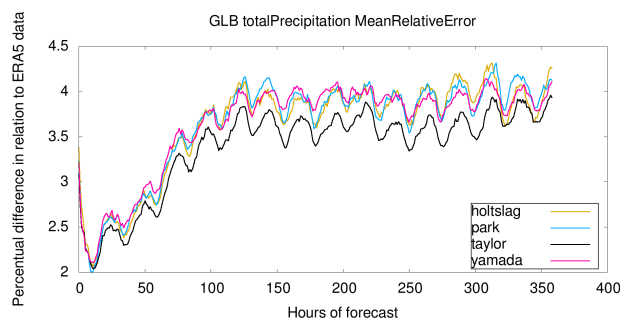
Figure 12. Global Total Precipitation, MRE from BAM simulation at TQ126 in dry season compared to ERA5 reanalysis data.

5.3 Wet Season

The wet season maintained Taylor PBL parameterization best results in relation to the dry season consistently, however the results with the other PBL parameterization schemes were more similar to Taylor PBL parameterization. In the global and Amazonian scenarios, Taylor PBL parameterization presented the most relevant results, while for South America in general, no improvements were obtained.

### 5.3.1 Time Mean Temperature at 2m

During the wet season, the temperature at 2 meters was best simulated in the Amazon basin by the BAM model using Taylor PBL parameterization (Table 4). It can be verified in Figure 13 that the best results come in the first simulated week, where the temperatures have their smallest variations in the Taylor results. However, a general analysis in Figure 13 makes it difficult to determine which is the best parameterization option for the boundary layer of the BAM model to simulate the temperature at 2 meters in the Amazon region.

14
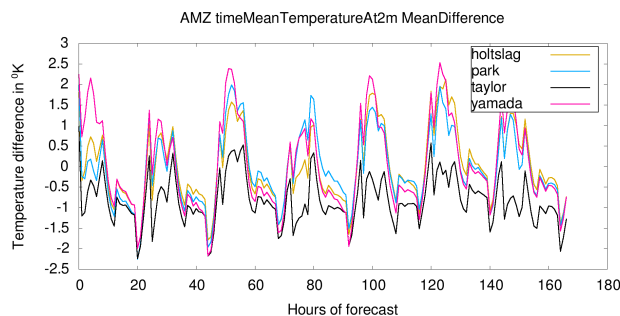
Figure 13. Time Mean Temperature at $2m$ in the Amazon basin, MD from BAM simulation at TQ62 in wet season compared to ERA5 reanalysis data.

5.3.2 Planetary Boundary Layer Height

The height of the PBL was not best simulated by the Taylor parameterization in most regions, but at the Amazon basin region in the rainy season it got a little closer to the reanalysis data again. In this region, the Taylor parameterization obtained the
270   second lowest error, with Park parameterization in first place, as shown in Figure 14 and Table 4.
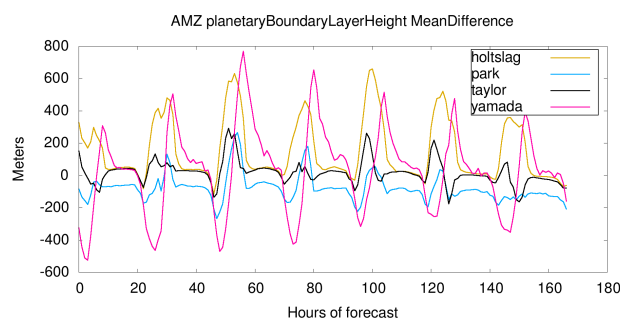
Figure 14. Planetary Boundary Layer Height in the Amazon basin, MD from BAM simulation at TQ62 in wet season compared to ERA5 reanalysis data.

5.3.3 Outgoing Long Wave at Top

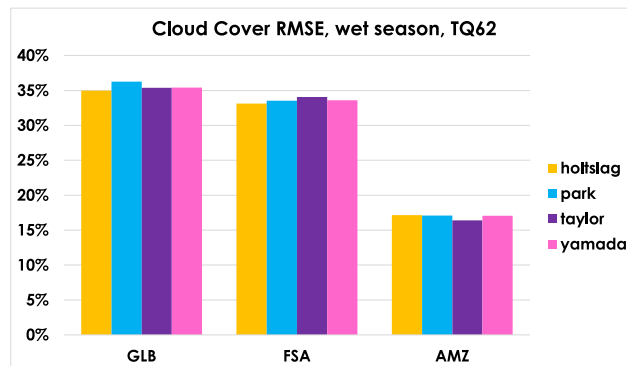When Taylor PBL parameterization is used in simulations with BAM, the thermal radiation at the top of the atmosphere is the variable that presents the smallest error in relation to the ERA5 reanalysis data. Figure 15 shows the average difference between the model and ERA5 data, where a small error can be seen in the simulation using Taylor in relation to the other
275   boundary layer schemes of the BAM model.

15
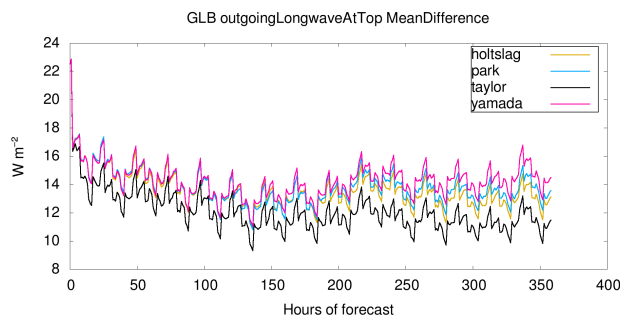
Figure 15. Global Outgoing Long Wave at Top, MD from BAM simulation at TQ126 in wet season compared to ERA5 reanalysis data.

5.3.4 Cloud Cover

The cloud cover did not have a significant improvement when using the Taylor parameterization in the simulations for the wet season. The model skill only improves for dry season period simulations. In the Amazon basin region there is only a small improvement in the simulation of the cloud cover field, as illustrated in Figure 16.

Figure 16. Cloud Cover, RMSE from BAM simulation at TQ62 in wet season compared to ERA5 reanalysis data in the three geographic ranges.

5.3.5 Total Precipitation

The precipitation simulated by the model with Taylor PBL parameterization in the rainy season did not approach the ERA5 reanalysis data as it did in the dry season in South America and in the Amazon, but maintained its global performance, as seen in Figure 17, the MRE demonstrates that parameterization of Taylor is better by the end of the second week.
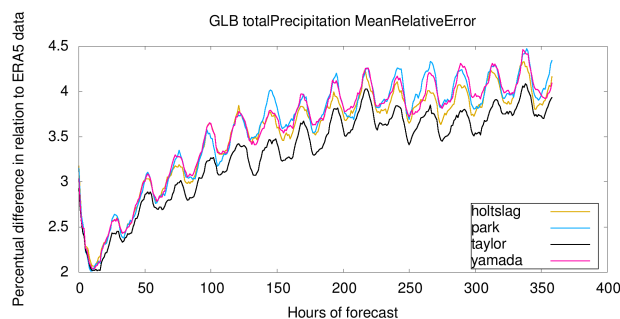
Figure 17. Global Total Precipitation, MRE from BAM simulation at TQ126 in wet season compared to ERA5 reanalysis data.

Table 2. BAM TQ126 RMSE Global averages for each simulation variable. The bold value is the smallest error in each column, compared to the ERA5 reanalysis data.

		dry season			
Method	timeMeanTemperatureAt2m	planetaryBoundaryLayerHeight	outgoingLongwaveAtTop	cloudCover	totalPrecipitation
HOLTSLAG	3.43ºK	**416m**	35.46Wm^{-2}	38.22%	12.52$\mathrm{kg(m^2\ day)}^{-1}$
PARK	**3.19ºK**	601m	35.19Wm^{-2}	39.91%	12.49$\mathrm{kg(m^2\ day)}^{-1}$
TAYLOR	3.80ºK	494m	**34.40Wm^{-2}**	**37.70%**	**11.99$\mathrm{kg(m^2\ day)}^{-1}$**
YAMADA	3.61ºK	535m	35.71Wm^{-2}	39.05%	12.43$\mathrm{kg(m^2\ day)}^{-1}$
		wet season			
Method	timeMeanTemperatureAt2m	planetaryBoundaryLayerHeight	outgoingLongwaveAtTop	cloudCover	totalPrecipitation
HOLTSLAG	4.50ºK	**385m**	34.72Wm^{-2}	37.68%	12.76$\mathrm{kg(m^2\ day)}^{-1}$
PARK	**4.08ºK**	569m	34.58Wm^{-2}	39.39%	12.88$\mathrm{kg(m^2\ day)}^{-1}$
TAYLOR	4.67ºK	469m	**34.05Wm^{-2}**	**37.53%**	**12.32$\mathrm{kg(m^2\ day)}^{-1}$**
YAMADA	4.64ºK	471m	35.12Wm^{-2}	38.39%	12.75$\mathrm{kg(m^2\ day)}^{-1}$

5.4 Global results

285   The global averages of the RMSE results for all the five variables shown in the Table 2, were consistent in both seasons, synthesizing the individual results analysed so far showing a good performance of the Taylor's parameterization in the Outgoing Long Wave at Top, Cloud Cover, and Total Precipitation in the end of the two weeks simulated by the BAM model. Considering a solid second place for the method at PBL height and at least consistent results for Mean Temperature at 2 meters, that is a favorable result for the Taylor's PBL parameterization towards seasonal and climate simulations.

Geoscientific
Model Development
Discussions

Table 3. BAM TQ126 RMSE Full South America averages for each simulation variable. The bold value is the smallest error in each column, compared to the ERA5 reanalysis data.

			dry season		
Method	timeMeanTemperatureAt2m	planetaryBoundaryLayerHeight	outgoingLongwaveAtTop	cloudCover	totalPrecipitation
HOLTSLAG	3.02ºK	**422m**	37.42Wm^{-2}	38.98%	13.23$\text{kg(m}^2\text{ day)}^{-1}$
PARK	**2.83ºK**	586m	37.64Wm^{-2}	41.02%	13.19$\text{kg(m}^2\text{ day)}^{-1}$
TAYLOR	3.40ºK	493m	**36.60Wm^{-2}**	**38.08%**	**12.22$\text{kg(m}^2\text{ day)}^{-1}$**
YAMADA	3.23ºK	533m	38.85Wm^{-2}	39.90%	12.79$\text{kg(m}^2\text{ day)}^{-1}$
			wet season		
Method	timeMeanTemperatureAt2m	planetaryBoundaryLayerHeight	outgoingLongwaveAtTop	cloudCover	totalPrecipitation
HOLTSLAG	2.90ºK	**418m**	40.33Wm^{-2}	**37.10%**	15.54$\text{kg(m}^2\text{ day)}^{-1}$
PARK	**2.68ºK**	567m	**39.79Wm^{-2}**	37.95%	15.28$\text{kg(m}^2\text{ day)}^{-1}$
TAYLOR	3.33ºK	484m	39.95Wm^{-2}	37.42%	14.71$\text{kg(m}^2\text{ day)}^{-1}$
YAMADA	3.13ºK	491m	40.63Wm^{-2}	37.56%	**14.62$\text{kg(m}^2\text{ day)}^{-1}$**

5.5 Full South America results

The South America scenario brought some difficulties for the presented method to reproduce the reanalysis data, specially in the wet season. The overall loss of performance in the wet season is visible in the Table 3 alongside the consistent good performance in the dry season, repeating similar results to those previously seen in the global simulations. Taylor's parameterization holds the second place in the wet season, together with the good dry season performance it stills a considerable option.

5.6 Amazon basin results

The Amazon basin got the closest results to the reanalysis when simulated using Taylor's PBL parameterization. In the Table 4, the dry season good performance is still visible alongside a new good result in the Mean Temperature at 2 meters (in both seasons), only observed in the Amazon results. The method gather some good results even in the wet season, differently than the Full South America experiment, proving its utility in weather forecast or future studies about the climatology in the Amazon region.

6 Conclusions

This article brought the first results with the implemented PBL turbulence parameterization based on Taylor's theory for all PBL stability conditions in the BAM model. This new boundary layer closure scheme implemented in the model takes into account physical processes such as the maximum of the turbulent kinetic energy spectrum and Kolmogorov's Law of $-5/3$ in

Table 4. BAM TQ126 RMSE Amazon averages for each simulation variable. The bold value is the smallest error in each column, compared to the ERA5 reanalysis data.

dry season					
Method	timeMeanTemperatureAt2m	planetaryBoundaryLayerHeight	outgoingLongwaveAtTop	cloudCover	totalPrecipitation
HOLTSLAG	3.03°K	500m	37.27Wm^{-2}	40.91%	13.80$\mathrm{kg(m^2\ day)}^{-1}$
PARK	3.53°K	**383m**	37.44Wm^{-2}	42.51%	14.51$\mathrm{kg(m^2\ day)}^{-1}$
TAYLOR	**2.52°K**	408m	**35.23Wm^{-2}**	**38.44%**	**12.57$\mathrm{kg(m^2\ day)}^{-1}$**
YAMADA	3.82°K	742m	39.37Wm^{-2}	40.45%	12.81$\mathrm{kg(m^2\ day)}^{-1}$
wet season					
Method	timeMeanTemperatureAt2m	planetaryBoundaryLayerHeight	outgoingLongwaveAtTop	cloudCover	totalPrecipitation
HOLTSLAG	2.10°K	336m	60.84Wm^{-2}	19.39%	22.88$\mathrm{kg(m^2\ day)}^{-1}$
PARK	2.18°K	**273m**	60.67Wm^{-2}	**19.16%**	22.69$\mathrm{kg(m^2\ day)}^{-1}$
TAYLOR	**2.04°K**	287m	**60.47Wm^{-2}**	19.60%	21.42$\mathrm{kg(m^2\ day)}^{-1}$
YAMADA	2.27°K	365m	61.99Wm^{-2}	20.07%	**21.02$\mathrm{kg(m^2\ day)}^{-1}$**

305 the inertial subdomain of the spectrum. The results with the new parameterization were confronted with the results achieved using PBL schemes presented by Holtslag-Boville, Sungsu-Park, and Mellor-Yamada when compared to the ERA5 reanalysis data, with a set of simulations in the BAM model using two different resolutions (a lower resolution one week simulation and a higher resolution two weeks simulation) in two different seasons (dry and wet), evaluating five different simulation variables in three different geographic ranges (global, South America, and Amazon). The results observed were positive for the new

310 PBL parameterization, specially in the dry season, on the Outgoing Long Wave at Top, Cloud Cover, and Total Precipitation variables, in all the three geographic regions.

A good representation of atmospheric radiation in a climate model is essential for successful climate simulations (COELHO et al., 2021). The amount of radiation at the top of the atmosphere is a good indicator of the energy balance in the simulation, and the overall good result for this variable while using Taylor's parameterization is a positive indication towards a good energy

315 balance within the method.

The good performance reproducing the reanalysis data in the Global scale points to future uses of Taylor's parameterization in climate models or initial condition generation for local forecast models.

The results were also positive for the Amazon basin region, simulating well not only the three variables globally well performed, but also the Mean Temperature at 2 meters. Good approximations in this region are an appreciated result considering

320 the importance of the Amazon forest's evapotranspiration in precipitation (YANG, 2019) and influence in the weather forecast on its neighbour regions, particularly important for precipitation in the southeast part of Brazil (LEMES et al., 2020).

Geoscientific
Model Development
Discussions

Open Access

EGU

Find positive results using the Taylor's PBL parameterization can be useful beyond the model raw results itself, for instance, good data from a global model are appreciated as initial condition for regional models. Considering all the different results analysed, as part of a future research, a multi-model ensemble using all the four PBL parameterization can be evaluated attributing a weight to each method according to the results gathered in this work, valuing each region, season, or perhaps simulation variable, with a proper parameterization to maximize the simulation accuracy. One technique for estimating multi-model forecast weights is based on an inverse problem formulation, as applied by Santos (2013) and Luz (2015). As a future work, the implementation of a counter-gradient parameter in the Taylor's parameterization will be investigated to seek for better accuracy simulating a downward turbulent flow of heat, moist and wind during the convective phase of the PBL.

Code availability. The modified source files from the BAM model and the scripts used to generate the results are available at https://doi.org/10.5281/zenodo.7681528.

Author contributions. HFCV developed the the theory and deduced the equations, PYK set up the model, PYK and ERE coded the parameterization, ERE designed and performed the experiments, ERE and HFCV wrote the paper, PYK and HFCV reviewed the paper.

Competing interests. The authors declare that they have no conflict of interest.

References

340   AMS. Glossary of Meteorology. Accessed ar: https://glossary.ametsoc.org/wiki/Slab_model.

BARBOSA, J. P. S., CAMPOS VELHO, H. F., FREITAS, S. R.: Implementação de Novas Parametrizações de Turbulência no BRAMS. Ciência e Natura, v. 111, 301-305, 2007.

BATCHELOR, GEORGE. K., "Diffusion in a Field of Homogeneous Turbulence, Eulerian Analysis", Australian Journal of Scientific Research, Vol. 2, p. 437-450, 1949.

345   BATCHELOR, GEORGE. "The Life and Legacy of G. I. Taylor", Cambridge University Press, 2008.

BRETHERON, CHRISTOPHER S., and SUNGSU PARK. "A new moist turbulence parameterization in the Community Atmosphere Model". Journal of Climate, vol. 22, no. 12, p. 3422-3448, 2009.

CAMPOS VELHO, H. F.: Modelagem Matemática em Turbulência Atmosférica. Sociedade Brasileira de Matemática Aplicada e Computacional (SBMAC): Notas em Matemática Aplicada - No. 48, 2010.

350   CARVALHO, J. C., DEGRAZIA, G. A., ANFOSSI, D., CAMPOS, C. R. J., ROBERTI, D. R., KERR, A. S.: Lagrangian stochastic dispersion modelling for the simulation of the release of contaminants from tall and low sources Meteorologische Zeitschrift, v. 11, n. 2, 89-97, 2002.

COELHO, CAIO AS, DAYANA C. de SOUZA, PAULO Y. KUBOTA, SIMONE COSTA, LAYRSON MENEZES, BRUNO S. GUIMARÃES, SILVIO N. FIGUEROA et al. "Evaluation of climate simulations produced with the Brazilian global atmospheric model version 1.2". Climate Dynamics 56, no. 3, p. 873-898, 2021.

355   DEGRAZIA, G. A.; MORAES, O. L. L. A model for eddy diffusivity in a stable boundary layer. Boundary-Layer Meteorology, v. 58, n. 3, p. 205-214, 1992.

DEGRAZIA, G. A.; CAMPOS VELHO, H. F.; CARVALHO, J. C.; Nonlocal Exchange Coefficients For The Convective Boundary Layer Derived From Spectral Properties. Beiträge zur Physic der Atmosphäre, v. 70, n.1, 57-64, 1997.

DEGRAZIA, G. A.; ANFOSSI, D.; CARVALHO, J. C.; MANGIA, C.; TIRABASSI, T; CAMPOS VELHO, H. F.; Turbulence parameteri-
360   zation for PBL dispersion models in all stability conditions. Atmospheric Environment, v. 34, p. 3575-3583, 2000.

FIGUEROA, S. N.; BONATTI, J. P.; KUBOTA, P. Y.; GRELL, G. A.; MORRISON , H.; BARROS, S. R.; FERNANDEZ, J. P.; RAMIREZ, E.; SIQUEIRA, L.; LUZIA, G. et al. The Brazilian global atmospheric model (BAM): Performance for tropical rainfall forecasting and sensitivity to convective scheme and horizontal resolution, Weather and Forecasting, v. 31, p. 1547û1572, 2016.

FOKEN, T.: Micrometeorology. 2nd Edition, Springer. 2017.

365   FOLEY, JONATHAN A. et al. An integrated biosphere model of land surface processes, terrestrial carbon balance, and vegetation dynamics. Global biogeochemical cycles, v. 10, n. 4, p. 603-628, 1996.

FUNCEME. Fundação Cearense de Meteorologia e Chuvas Artificiais. Accessed at: http://www.funceme.br/.

HERSBACH, H., BELL, B., BERRISFORD, P., BIAVATI, G., HORÁNYI, A., MUÑOZ SABATER, J., NICOLAS, J., PEUBEY, C., RADU, R., ROZUM, I., SCHEPERS, D., SIMMONS, A., SOCI, C., DEE, D., THÉPAUT, J-N. ERA5 hourly data on single levels from 1959 to
370   present. Copernicus Climate Change Service (C3S) Climate Data Store (CDS). (Accessed on Dec-13-2022), 10.24381/cds.adbb2d47. 2018.

HOLTSLAG, A.; BOVILLE, B. A.; Local versus nonlocal boundary-layer diffusion in a global climate model. Journal of Climate, v. 6, n. 10, 1825û1842, 1993.

KAIMAL, J. C.; WYNGAARD, J. C. The kansas and minnesota experiments. Boundary-Layer Meteorology, v. 50, n. 1, p. 31-47, 1990.

375   LEMES, M.D.C.R., de OLIVEIRA, G.S., FISCH, G., TEDESCHI, R.G. and da SILVA, J.P.R. Analysis of moisture transport from Amazonia to Southeastern Brazil during the austral summer. Revista Brasileira de Geografia Fϕsica, 13(06), pp.2650-2670. 2020.

LUZ, E. F. P., SANTOS, A. F., FREITAS, S. R., CAMPOS VELHO, H. F., GRELL, G. A.: Optimization by firefly with predation for ensemble precipitation estimation using BRAMS. American Journal of Environmental Engineering, v. 5, n. 1A, 27-33, 2015.

MELLOR, G. L.; YAMADA, T;: Development of a turbulence closure model for geophysical fluid problems. Reviews of Geophysical Physics
380   and Space Physics, v. 20, 851-875, 1982.

MONNA, W. A. A.; VAN DER VLIET, J. G. Facilities for research and weather observations on the 213 m tower at Cabauw and at remote locations. De Bilt, The Netherlands: KNMI, 1987.

MOREIRA, V. S., DEGRAZIA, G. A., ROBERTI, D. R., TIMM, A. U., CARVALHO, J. C.; Employing a Lagrangian stochastic dispersion model and classical diffusion experiments to valuate two turbulence parameterization schemes. Atmospheric Pollution Research, v. 2,
385   384-393, 2011.

OLESEN, H. R.; LARSEN, Søren Ejling; HØJSTRUP, Jørgen. Modelling velocity spectra in the lower part of the planetary boundary layer. Boundary-Layer Meteorology, v. 29, n. 3, p. 285-312, 1984.

ONS. Operador Nacional do Sistema Elétrico. Accessed at: https://www.ons.org.br/.

NIEUWSTADT, F. T. M. Nieuwstadt, The turbulent structure of the stable nocturnal boundary layer. Journal of the Atmospheric Sciences, v.
390   41, 2202–2216, 1984.

RANDALL, David DAVID A.; PAN, DZONG-MING. Implementation of the Arakawa-Schubert cumulus parameterization with a prognostic closure. In: The representation of cumulus convection in numerical models. American Meteorological Society, Boston, MA, 1993.

RIZZA, U., DEGRAZIA, G. A., MOREIRA, D. M. , BRAUER, C. R. N. , MANGIA, C., CAMPOS, C. R. J., TIRABASSI, T.: Turbulent dispersion from tall stack in the unstable boundary layer: A comparison between Gaussian and K-diffusion modelling for nonbuoyant
395   emissions. Il Nuovo Cimento, Vol. 24-C, N. 6, 805–814, 2001.

ROBERTI, R. R., SOUTO R. P., CAMPOS VELHO H. F., DEGRAZIA, G. A., ANFOSSI, D.; Parallel Implementation of a Lagrangian Stochastic Model for Pollutant Dispersion. Journal of Parallel Programming, v. 33, n.5, 485–498, 2005.

ROBERTI, R. R., ANFOSSI, D., CAMPOS VELHO H. F., DEGRAZIA, G. A., Estimation of emission rate from experimental data. IL Nuovo Cimento, v. 30-C, n. 2, 177-186, 2007.

400   ROBERTS, P. J. W.; WEBSTER, D. R., "Turbulent Diffusion" (Chapter), in extitEnvironmental Fluid Mechanics: Theories and Applications (Editors: H. H. Shen, A. H. D. Cheng, K-H Wang, M. H. Teng, C. C. K. Liu), ASCE Press (Reston, Virginia, USA), 2002.

SCHÜNZEN, K. H.: Mesoscale Modelling in Complex Terrain – An Overview on the German Nonhydrostatic Models. Meteorologische Zeitschrift, v. 67, n. 3, 243-253, 1994.

SANTOS, A. F., FREITAS, S. R., MATTOS, J. G. Z., CAMPOS VELHO, H. F., GAN. M. A., LUZ, E. F. P., GRELL: Using the firefly
405   optimization method to weight an ensemble of rainfall forecasts from the Brazilian developments on the Regional Atmospheric Modeling System (BRAMS). Advances in Geosciences, v. 35, 123–136, 2013.

STULL, R. B.: An Introduction to Boundary Layer Meteorology, Springer Science & Business Media, 1988.

TARASOVA, T. A.; FOMIN, B. A. The use of new parameterizations for gaseous absorption in the CLIRAD-SW solar radiation code for models. Journal of Atmospheric and Oceanic Technology, v. 24, n. 6, p. 1157-1162, 2007.

410   TAYLOR, GEOFFREY I. Diffusion by continuous movements. Proceedings of the London Mathematical Society 2, no. 1, 1922.

XUE, Y.; ZENG, F.; SCHLOSSE, C. A simplified Simple Biosphere Model (SSiB) and its application to land-atmosphere interactions. 1991.

YANG, Z., and DOMINGUEZ, F. "Investigating Land Surface Effects on the Moisture Transport over South America with a Moisture Tagging Model". Journal of Climate 32.19 (2019): 6627-6644. < https://doi.org/10.1175/JCLI-D-18-0700.1>. Web. 26 Jan. 2023.